Effects of the impact angle on the coefficient of restitution based on a medium-scale laboratory test

Yanhai Wang[1], Wei Jiang[1,2], Shengguo Cheng[2] , Pengcheng Song[2] ,Cong Mao[2]

[1] Hubei Key Laboratory of Disaster Prevention and Mitigation (China Three Gorges University), Yichang, Hubei, 443002, People's Republic of China

[2] Department of Civil, Structural, and Environmental Engineering, University at Buffalo, Buffalo, NY, 14260, United States

Correspondence to: Wei Jiang (jiangweilion@163.com)

Abstract. The reliability of a computer program simulating rockfall trajectory depends on the ascertainment of reasonable values for the coefficients of restitution, which typically vary with the kinematic parameters and terrain conditions. The effects of the impact angle with respect to the slope on the coefficients of restitution have been identified and studied using small scale laboratory tests. To investigate whether the existing conclusion based on small scale laboratory tests is valid when the test scale changes and the role of rotation in the effect of the impact angle on the coefficients of restitution, this study performed a medium-scale laboratory test using spherical limestone polyhedrons impacting concrete slabs. Free fall test are conducted and the velocities before and after the impact are obtained by a 3D motion capture system. The result comparison between our test and the existing small scale tests verified that several general laws occur when accounting for the effect of the impact angle, regardless of the test scales and conditions. Increasing the impact angle will induce reductions in the normal coefficient of restitution R_n, the kinematic coefficient of restitution R_v and the kinetic energy coefficient of restitution R_E, whereas it will lead to increases in the tangential coefficient of restitution R_t. The rotation plays an important role in the effect of the impact angle. A higher percentage of kinetic energy converted to rotational energy always induces a higher normal coefficient of restitution R_n and a lower tangential coefficient of restitution R_t. The percentage of kinetic energy converted to rotational energy during the collision increases as the impact angle decreases, and large samples are more likely to have a stead and small percentage than small samples.

1 Introduction

In mountain areas, rockfall is a frequent natural disaster that endangers human lives and infrastructure. Numerous examples of fatalities or infrastructure damage due to rockfall have been reported (Guzzetti, 2003; Pappalardo, 2014). Various protective measures, such as barrier fences, cable nets and rockfall shelters, have been widely used to reduce rockfall hazards. To ensure the efficiency of mitigation techniques, the motion trajectory of the rockfall must be estimated. The trajectory can provide important information, such as the travel distances of possible rockfall events, the bouncing height and kinetic energy level of the rockfall at various positions along the slope.

Numerous algorithms have been developed to solve this problem, and the progress up to the end of the last century has been summarized by Dorren (2003) and Heidenreich (2004). Due to these efforts, computer simulation codes, such as RockFall (Stevens, 1998), CRSP (Jones et.al, 2000) and Stone (Guzzetti et.al, 2002), RAMMS::Rockfall (Christen et al, 2007), Rockyfor3D (Dorren, 2010) and Pierre (Valentin et al., 2015; Andrew and Oldrich, 2017), are developed to acquire motion information for rockfall. A main feature that allows one to distinguish between different rockfall trajectory codes is the representation of the objective rock. The first approach, a lumped-mass model, treats the rock as a single and dimensionless point, and assigns all of the properties of the rock to that point. The second one is a rigid body model, which considers the rock as a body with its own shape and volume, and accounts for all types of block movement, including rotation. Finally, a hybrid model adopts a lumped mass model to calculate the free flight of the rock, and simulates the rebound, rolling or sliding using a rigid body model. In those codes, the most crucial input parameter determining the rockfall trajectory is the coefficient of restitution, which is used to control the rebound motion, a succession of rockfalls impacting the slope surface.

1.1 Definition for the coefficient of restitution

The coefficient of restitution is a dimensionless value representing the ratio of velocities or energies of a boulder before and after it impacts the slope. Various definitions for the coefficient of restitution have been proposed in previous studies, but no consensus was reached on which definition is more appropriate for rockfall prediction. As shown in Fig. 1, when one boulder impacts the slope surface, the impact velocity v_i can be resolved into a normal component v_{ni} and a tangential component v_{ti} according to the slope angle θ. Then, the boulder leaves the surface with a rebound velocity v_r, which similarly has a v_{nr} and a v_{tr}. The angular velocities of the boulder before and after impact are denoted as ω_i and ω_r, respectively. The impact angle α and rebound angle β are drawn in Fig. 1.

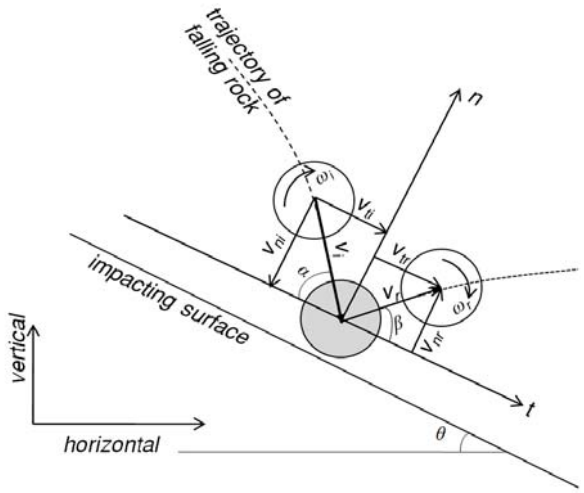

Fig. 1. Related quantities adopted in definitions for the coefficient of restitution

The normal and tangential coefficients of restitution are the most used definitions, and these coefficients of restitution are typically denoted as R_n and R_t, respectively. The mathematical expressions of R_n and R_t are

$$R_n = v_{nr} / v_{ni}, R_t = v_{tr} / v_{ti} \quad (1)$$

Another common definition is the kinematic coefficient of restitution, R_v, representing the ratio between the magnitudes of the rebound and impact velocities:

$$R_v = v_r / v_i \quad (2)$$

This definition originated from Newton's theory of particle collision, and had been used by Habib (1976), Paronuzzi (1989) and other scholars. When R_v is used in the trajectory predication, an assumption regarding the rebound direction is necessary to fully determine the velocity vector after impact.

In addition, the ratio of kinetic energies before and after impact is used to define the kinetic energy coefficient of restitution R_E, which is written as

$$R_E = E_r / E_i = (E_{rr} + E_{rt}) / (E_{ir} + E_{it}) \quad (3)$$

in which E_i and E_r are the kinetic energy before and after the impact, respectively. E_{rr} and E_{ir} are the rotational energy before and after the impact; E_{it} and E_{rt} denote the translational energy before and after the impact. E_{ir}, E_{it}, E_{rr} and E_{rt} are computed as

$$E_{ir} = 0.5 I \omega_i^2, E_{it} = 0.5 m v_i^2, E_{rr} = 0.5 I \omega_r^2, E_{rt} = 0.5 m v_r^2 \quad (4)$$

Here, m is the mass, I is the moment of inertia. R_E can reflect the kinetic energy loss caused by the impact, and had been used by Bozzolo and Pamini (1986), Azzoni et al. (1995) and Chau et al. (2002).

In these definitions, R_n and R_t got more popularity in engineering practice for the simplicity in computer simulation software. R_n and R_t are used conjointly and characterize the variation in the tangential and normal components of the boulder velocity, respectively. Given an impact velocity, the rebound velocity and direction can be completely determined using this definition without any further assumption. So, R_n and R_t attracted most attentions in the previous studies, and some typical values of R_n and R_t had been summarized (Agliardi and Crosta, 2003; Heidenreich, 2004; Scioldo, 2006).

1.2 Previous studies on the effects of the impact angle on the coefficient of restitution

Various techniques, such as laboratory tests (Buzzi et.al, 2012; Asteriou et.al, 2012), field tests (Dorren et.al, 2006; Spadari et al. 2012), back analysis of field evidence (Paronuzzi, 2009) and theoretical estimation (He et.al, 2008), have been used to determine the coefficient of restitution. Variations in the impact conditions, e.g., the material properties of both the rocks and slopes (Wu, 1985; Fornaro et.al, 1990; Robotham et.al, 1995; Richards et.al, 2001; Chau et.al, 2002; Asteriou et.al, 2012), the shape of the rocks (Chau et.al, 1999; Buzzi et.al, 2012), the roughness of the slope surface (Giani et.al, 2004) and the impact angle, influence the coefficient of restitution considerably. While, in those summaries for typical values of coefficient of restitution, they were determined only accounting for the terrain conditions.

The impact angle, the angle between the directions of the impact velocity and the slope segment, is a kinematic parameter of the falling rock, indicating only that the terrain conditions involved in estimating the value of the coefficient of restitution may be unreliable. Since Broili (1973) first identified this problem, numerous experiments have been performed to acquire a comprehensive picture of the effects of the impact angle. In situ tests are expensive and not suitable for statistical and

parameter analysis; thus, existing studies have largely been performed in the laboratory. In some literatures, the impact angle was referred to as the slope angle θ (or the impact surface angle) in free-fall tests. While, the impact surface angle is only another expression because the slope angle θ and impact angle α sum up to 90° under these conditions.

Wu (1985) conducted laboratory tests using rock blocks on a wooden platform and rock slope, and suggested that there is a linear correlation between the impact surface angle and the mean value of the restitution coefficient. He proposed that increasing the angle of the impact surface causes the normal coefficient R_n to increase regardless of the block mass and causes the tangential coefficient R_t to decrease slightly.

Richards et al. (2001) executed free-falling tests considering different types of rock and slope conditions and established a correlation between the coefficient of restitution and the Schmidt hammer rebound hardness. The impact surface angle was added to the correlation to reflect its linear improvement effect on the normal coefficient R_n.

Chau et al. (2002) conducted experiments using spherical boulders and a rock slope platform, both made of dental plaster. The free-falling tests indicated that the normal coefficient increases with increases in the impact surface angle, whereas there was no clear correlation with the tangential coefficient.

Cagnoli and Manga (2003) studied oblique collisions of lapilli-size pumice cylinders on flat pumice targets and determined that the impact angle can influence the rebound angle, the kinetic energy loss and the ratios of the velocity components. The normal coefficient decreases as the impact angle approaches 90°.

Asteriou et al. (2012) performed laboratory tests using five types of rocks from Greece. The result of the parabolic drop tests indicated that the kinematic coefficient of restitution R_v was more appropriate than the normal coefficient of restitution for use in correlations with the impact angles. Then, the normal coefficient of restitution could be estimated accounting for the rebound–impact angle ratio.

Buzzi et al. (2012) conducted experiments using flat concrete blocks in four different forms and determined that a combination of low impact angle, rotational energy and block angularity may result in a normal coefficient of restitution in excess of unity.

James (2015) evaluated restitution coefficients using milled aluminium blocks and a planar wooden slope. Three different shapes of blocks were custom made and the slope surface was carpeted. Both the first impact under free fall conditions and the series impacts during runout were recorded. It was observed that R_n shows a positive correlation with increasing slope angle while R_t shows a negative correlation.

These efforts have highlighted the importance of the impact angle with regard to the coefficient of restitution. However, the common method in the existing laboratory tests was to capture the trajectory of a block using a high-speed video camera; meanwhile small samples were used. Therefore, the existing results are restrained by the small scale of the laboratory tests. Influence factors are much more than the material properties and sizes, which induces the absence of the matured similarity theory for the model test on the coefficient of restitution (Heidenreich, 2004). Thus, it is uncertain whether the test scale change the laws regarding the effect of the impact angle on the coefficient of restitution. In additional, the rotation plays an important role in kinetic energy dissipation during impact, but the studies on the rotational energy is rather limited (Chau et

al., 2002; Cagnoli and Manga, 2003). Whether a correlation occurs between the rotation and the effect of the impact angle on the coefficient of restitution isn't determined till now.

Hence, the current study employs a 3D motion capture system and a special releasing device to perform a medium-scale laboratory experiment. Spherical polyhedrons made of limestone were selected as samples, with a maximum diameter of 20 cm. The landing plate consisted of C25 concrete slabs. To address the effect of the impact angle, different inclined plate angles and releasing heights were used in free fall tests. The resulting coefficients of restitution were calculated, and the trends for R_n, R_t, R_t and R_E in terms of the impact angle were explored. Then, the results are compared with three existing small scale experiments to determine whether the test scale affects the law that the impact angle influences the coefficients of restitution. The percentage of the total kinetic energy before impact converted to rotational energy was investigated, and the role of rotation in the effect of the impact angle on the coefficient of restitution was analysed.

2 Laboratory investigation

2.1 Rock specimens and concrete slabs

All falling rock specimens in this study were natural limestone from the China Three Gouges area and were customized in accordance with the required sizes. As shown in Fig. 2a, irregular artificial cutting facets constituted the surface of the specimens, and the edges were not smoothed; thus, the shape is called a spherical polyhedron in this study to distinguish it from the standard sphere used in other research studies. To address the effect of rock size on the rebound characteristics, two different diameters were considered (D=10 cm and D=20 cm), with corresponding average masses of 1.2 kg and 10 kg. The C25 concrete slabs were produced in a prefabricated concrete factory. As shown in Fig. 2b, each concrete slab had dimensions of 1,200 mm×500 mm×150 mm. The mechanical properties of the materials adopted in test are determined beforehand. The limestone has the Young's modulus E=41 GPa, the Poisson's ratio v=0.21 and Schmidt Hardness R=36.0. And the concrete has E=28 GPa, v=0.20 and R=32.5.

(a) Limestone rocks

(b) Concrete slabs

Fig. 2. Materials used in this study

2.2 Testing apparatus

The apparatus used in this study consisted of a ramp, landing plate and releasing device (Fig. 3a). The ramp was built by compacting gravelly soil and had an inclined surface with planned angles produced by artificial excavation. Then, two concrete slabs were placed upon the inclined surface to form the landing plate. One device was designed and manufactured specially to catch and release specimens of various sizes. As shown in Fig. 3b, the device had four adjustable tongs at the bottom, which could grasp spherical blocks with diameters from 8 cm to 25 cm. A wireless receiver and electromagnetic relay were installed in the upper portion of the device, offering a wireless method of altering the tong status, grasping or loosing. The device could be connected to an indoor mobile crane by using the top ring, which means that the device could go up and down by managing the crane.

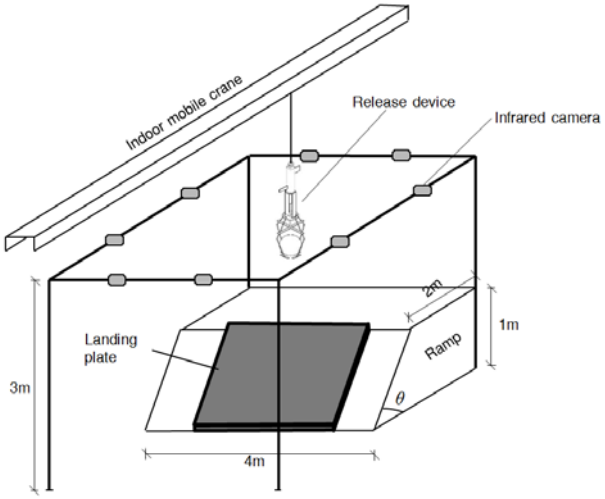

(a) General view

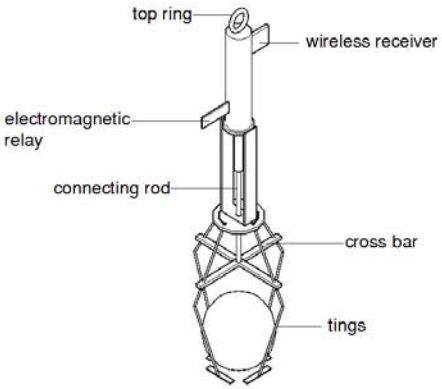

(b) Release device

(c) A falling block

(d) Damaged slabs to be replaced

Fig. 3. The testing apparatus

A free-fall test was performed in the experiment, and the complete process of one test is as follows. First, when one spherical polyhedron is prepared to be tested, the tongs are adjusted to accommodate the polyhedron by moving the cross bar up and down. After the sample is in the tongs, the grasping state is selected. Then, the device hanging on the indoor crane is moved to the position above the landing plate and lifted to the planned height. Next, by operating the wireless switch, the tongs are loosened, and the sample begins to fall (Fig. 3c). Finally, the sample impacts the landing plate, and its motion is recorded. The surface of the concrete slabs becomes worn with successive impacts. Once the surface occurs excessive damage as shown in Fig. 3d, the used slabs are replaced with new slabs.

2.3 Data acquisition

The spatial motion information of falling samples was obtained by the Doreal DIMS-9100(8c) Motion Capture System. This system has 8 near-infrared cameras (see Fig. 4a) with an operating speed of 60 fps and can capture the spatial trails of markers attached to the surface of the sample, as shown in Fig. 4b. Then, the motion analysis program provides the spatial motion information of the sample, e.g., its position and velocity. Finally, the coefficient of restitution can be calculated according to Eqs. (1)-(4) for subsequent analysis.

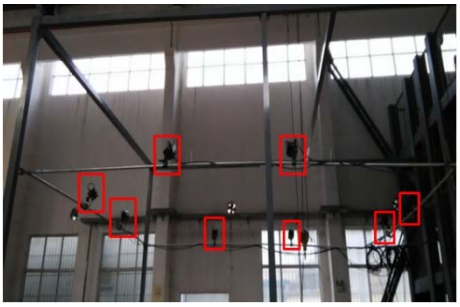

(a) Distribution of 8 infrared cameras

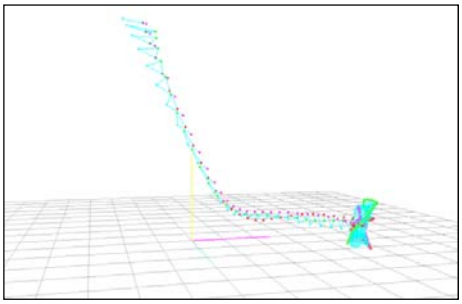

(b) Trails of marked points in one test

Fig. 4. Motion capture instruments

2.4 Experimental program

Four different inclined angles θ of the landing plate (30°, 45°, 60° and 75°) were considered in this study to determine the effect of the impact angle on the coefficients of restitution. The impact angles are approximately related to the incline angle θ of the landing plate under free-fall test conditions. Limestone specimens were released at three different heights of 2.5 m, 3.5 m and 4.5 m upon the inclined concrete slabs. The impact velocities varied from 6.7 to 9.3 m/s. While, two tests do not necessarily have identical release conditions even if they have the same release height and use the same specimen because the positions on which the tongs catch the specimen may differ slightly in any two tests.

In Table 1, the initial conditions of our experiment are presented, in addition to the resulting impact velocities and angles, R_n, R_t, R_v, R_E and the rebound angles. The inertia moment of the sample was approximated to a full sphere in the calculation of

rotational energy. Before impact, the angular velocities didn't exceed 3 rad/s, and the rotational energy of the rock only took up 0.01%-0.03% of the total kinetic energy in this study.

Table 1. Initial conditions and results of our experiments

Size (cm)	Inclined Angle θ (°)	Release Height (m)	Impact Velocities (m/s)		Impact Angles α (°)		R_n		R_t		R_v		R_E		Rebound Angles β (°)		Test Numbers N
			Mean	Std Dev	Mean	Std Dev	Mean	Std Dev	Mean	Std Dev	Mean	Std Dev	Mean	Std Dev	Mean	Std Dev	
10	30	2.5	6.50	0.11	57.25	1.41	0.42	0.09	0.80	0.03	0.56	0.04	0.36	0.05	38.31	6.21	4
		3.5	7.75	0.06	57.21	1.44	0.38	0.04	0.92	0.08	0.59	0.04	0.39	0.04	32.88	3.94	3
		4.5	9.06	0.16	58.27	1.33	0.39	0.03	0.88	0.04	0.57	0.01	0.37	0.02	35.49	3.23	3
	45	2.5	6.41	0.17	39.42	1.24	0.53	0.04	0.82	0.09	0.72	0.05	0.57	0.07	28.47	3.52	4
		3.5	7.72	0.09	39.07	0.66	0.52	0.02	0.78	0.08	0.69	0.06	0.52	0.08	28.48	2.85	3
		4.5	8.76	0.10	39.77	0.20	0.58	0.07	0.82	0.06	0.67	0.04	0.50	0.05	30.47	3.76	3
	60	2.5	6.51	0.21	25.06	1.21	0.76	0.06	0.69	0.03	0.70	0.03	0.59	0.04	27.17	1.77	3
		3.5	7.94	0.16	25.76	0.91	0.88	0.11	0.70	0.12	0.74	0.08	0.64	0.10	32.13	8.13	3
		4.5	8.80	0.17	26.99	1.62	0.53	0.17	0.70	0.02	0.67	0.02	0.51	0.03	20.92	5.70	3
	75	2.5	6.47	0.16	12.79	1.71	1.00	0.11	0.53	0.03	0.56	0.02	0.44	0.02	23.35	3.16	3
		3.5	7.91	0.08	10.06	0.73	1.11	0.27	0.65	0.19	0.67	0.17	0.58	0.21	18.65	7.38	3
		4.5	9.12	0.20	9.76	1.21	1.68	0.30	0.49	0.08	0.57	0.04	0.45	0.05	31.24	9.73	3
20	30	2.5	6.47	0.20	57.69	0.75	0.40	0.01	0.87	0.03	0.58	0.02	0.38	0.02	35.77	1.49	3
		3.5	7.80	0.11	58.09	1.44	0.31	0.03	0.89	0.11	0.54	0.03	0.34	0.02	29.41	4.18	3
		4.5	8.89	0.19	58.02	1.63	0.37	0.03	0.85	0.05	0.55	0.04	0.34	0.05	34.90	3.15	4
	45	2.5	6.47	0.21	40.97	3.14	0.56	0.03	0.73	0.02	0.66	0.02	0.53	0.04	33.89	4.48	3
		3.5	7.96	0.05	40.05	1.55	0.49	0.05	0.70	0.04	0.62	0.04	0.46	0.06	30.54	3.03	3
		4.5	8.74	0.13	40.16	0.22	0.47	0.09	0.86	0.04	0.72	0.04	0.56	0.05	24.68	3.77	3
	60	2.5	6.33	0.05	26.76	2.40	0.76	0.08	0.72	0.02	0.73	0.03	0.65	0.06	28.15	2.71	3
		3.5	7.57	0.09	24.96	0.38	0.74	0.13	0.66	0.07	0.68	0.05	0.56	0.07	27.64	5.60	3
		4.5	8.76	0.19	27.44	1.57	0.64	0.12	0.63	0.10	0.63	0.07	0.49	0.11	28.29	6.11	3
	75	2.5	6.08	0.16	11.39	1.52	0.79	0.07	0.67	0.13	0.71	0.09	0.65	0.09	14.32	5.67	3
		3.5	7.30	0.29	11.56	2.05	1.08	0.21	0.64	0.16	0.69	0.11	0.59	0.15	19.58	5.83	3
		4.5	7.97	0.26	10.63	2.90	1.17	0.18	0.62	0.16	0.68	0.12	0.58	0.15	19.41	3.23	3

3 Analysis of the results and comparison with existing studies

3.1 Effect of the impact angle on the coefficients of restitution based on our tests

Although the mean values and standard deviations have been calculated in terms of various release conditions, data points are considered in this section to provide a broad perspective for an evaluation of the effect of the impact angle. Four different inclined angles of the landing plate (θ=30°, 45°, 60° and 75°) induce four intervals of impact angles, 55°<α<60°, 36°<α<44°, 23°<α<30° and 6°<α<15°. The mean value of the coefficients of restitution are computed for the four intervals. In Fig. 5, solid lines are adopted to represent the mean values for samples with size D=10 cm, and dashed lines represent the mean values for size D=20 cm.

The effect of impact angle on the normal coefficient of restitution R_n is shown in Fig. 5a. When the impact angle is smaller than 15°, the values of R_n range from 0.709 to 1.989, and more than 60% of the values of R_n are larger than 1.0. A larger impact angle tends to produce a smaller value of R_n and reduce the discreteness. Initially the solid line is above the dashed line, although the gap narrows with increasing in the impact angle. When the impact angle is larger than 30°, these two lines do not exhibit a clear difference. Therefore, small specimens are more likely to have a high R_n than large specimens with small impact angles, and the effect of the rock size on R_n can be neglected when the impact angle is more than 30°.

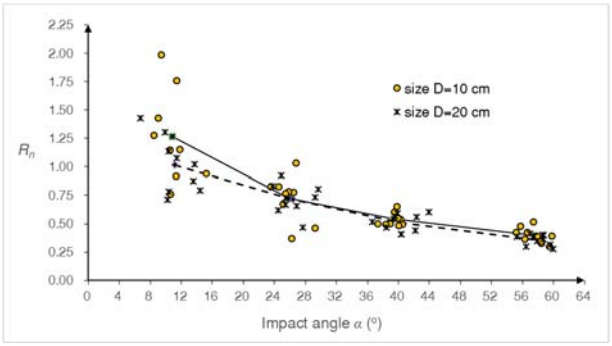

(a) R_n versus the impact angle a

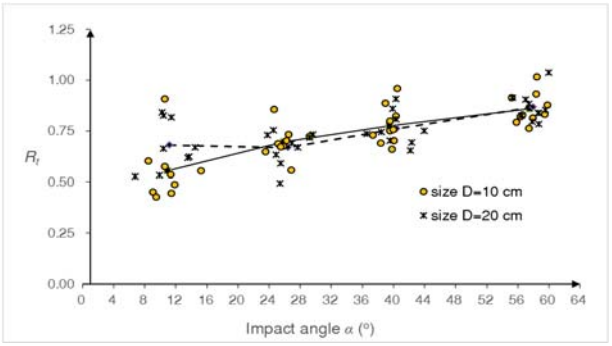

(b) R_t versus the impact angle a

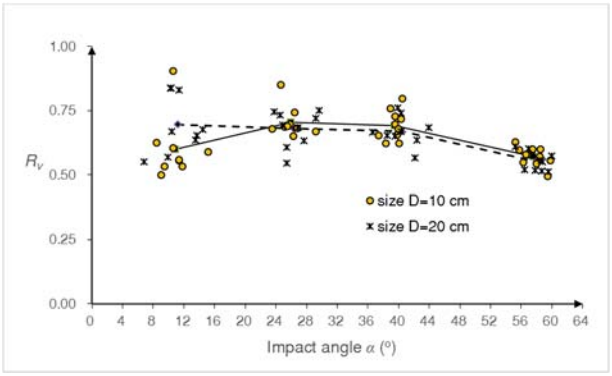

(c) R_v versus the impact angle a

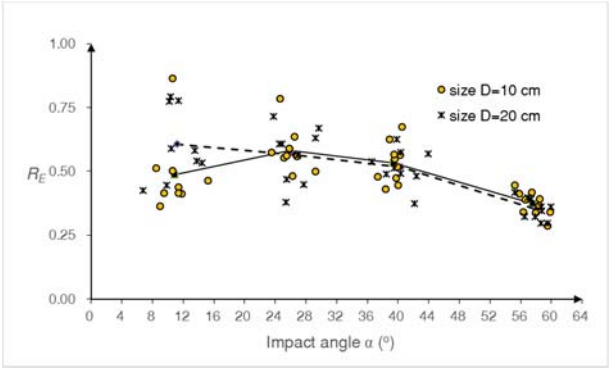

(d) R_E versus the impact angle a

Fig. 5. Effect of the impact angle on the coefficients of restitution

As Fig. 5b shows, the impact angle has a different effect on the tangential coefficient of restitution R_t than on R_n. In the first place, the discreteness of data points hasn't been reduced as the impact angle increases. Then, R_t increases slightly with increasing in the impact angle. In the first impact angle interval, the solid line is below the dashed line, which implies that small specimens gain a lower R_t than large specimens with small impact angles. Until the impact angle reaches 23°, the two lines have no distinct difference to be distinguished. Overall, the mean value lines in Fig. 5b seem to accord with the linear correlation between R_t and the impact angle α (Wu, 1985).

Furthermore, the kinematic coefficient of restitution R_v versus the impact angle is plotted in Fig. 5c. As the impact angle increases, the peak values of R_v of the four impact angle intervals fall down gradually, and R_v become concentrated. However, the mean values present a more complicated trend in Fig. 5c. Except that the solid line rises from the first impact angle interval to the second, the mean values have a decline in general. The decline is tiny from the second impact angle interval to the third, while it is apparent from the third to the fourth. Taking the small gap between the mean lines into account, bigger specimens are easier to gain a small R_v than small specimens when the impact angle is more than 23°.

Finally, the effect of the impact angle on the coefficient of kinetic energy restitution R_E is illustrated in Fig. 5d. Similar to Fig. 5c, the peak values of R_E of the four impact angle intervals decrease with increasing in the impact angle. But the discreteness of data points does not disappear clearly until the forth impact angle interval. The trends for the mean value of R_E are similar to R_v. However, the decline in the mean values of R_E is more intuitive than R_v from the second impact angle interval to the third. And the gap between the mean lines of R_E is narrower than R_v with larger impact angles. Although some scholars (Chau 2002; Asteriou 2012) suggested that smaller impact angles induce less kinetic energy loss and higher R_E, the deduction may be not suitable for small impact angles in this study.

Besides the effect of the impact angle on the four coefficients of restitution, other interesting phenomenon can be observed in Fig. 5. Two sizes are adopted in this experiment to evaluate the effect of rock size on the rebound characteristics. Except for smaller impact angle, the gaps between the two mean lines in Fig. 5 are much tiny compared to the magnitudes of restitution coefficients. Therefore, the four coefficients of restitution seem to be independent of the sample sizes in our test when the impact angle exceeds 23°, which could be attributed to the test conditions. As Farin et al. (2015) noted, the thickness of the impacted objective is an important factor in determining whether the coefficients of restitution change with the boulder size. When the impacted objective has a large thickness compared to the boulder size, the coefficient of restitution is independent of the boulder size. In this study, the impacted objective is concrete slabs fixed in the ground, which has enough thickness to eliminate the effect of rock size on the coefficients of restitution.

In addition, data points for all coefficients except R_t become concentrated as the impact angle increases. In the first impact angle interval, the diversity of R_n is clearly larger than the other three coefficients. However, when the impact angle exceeds 23°, the lowest diversity occurs for R_n, and the second is for R_v. Various functions have considered to match data points, but no function can provide a correlation coefficient R^2 more than 0.60 in terms of R_t, R_v and R_E for all options considered. Power function provides the best R^2 in matching data points of R_n, which reaches 0.80. So, the scaling law to describe data points is

abandoned in this study. Although Asteriou et al. (2012) suggested that R_v was more suitable than R_n for use in correlations with the impact angles, it is invalid in this study, which is caused by the variations of test conditions.

3.2 Comparison with existing small scale experiments

In this section, the effect of the impact angle on the coefficient of restitution obtained in this study is compared with some existing small scale experiments, to determine the effect of the test scale. Tests conducted by Chau et al. (2002), Cagnoli and Manga (2003), Asteriou et al. (2012) are selected here for data availability. The test conditions of those studies are provided in Table 2 in comparison with this study. This study mainly differs from the other studies in terms of the size and mass of the samples.

Table 2. Test conditions of the previous studies versus our experiment

	This study	Chau et al, 2002	Cagnoli and Manga, 2003	Asteriou et al., 2012
Sample shape	Spherical Polyhedron	Sphere	Cylinder	Cubic
Sample material	limestone	dental plaster	pumice	marble/sandstone/marl
Landing plate material	concrete	dental plaster	pumice	marble
Sizes (mm)	Diameter: 100/200	Diameter: 18.35/60/60	Basal diameter: 5.5 Length: 8.9	Edge:20
Mass (g)	1200/10000	6.05/153.64/204.33	0.11	19.9/20.3/16.5
Impact velocities (m/s)	6.7-9.3	4-5.65	24.88	3
Impact angles	6°-60°	20°-80°	18°-74°	16°-77°
Roughness of the target surface	uneven	flat	flat	smooth
Sharpness of the specimens	rear edges	no edges	rear edges	smooth edges

Although the previous studies imposed various test conditions, they provided references for us to evaluate the effect of the test scale. The effects of the impact angle on R_n, R_t, R_v and R_E provided by Chau et al. (2002), Cagnoli and Manga (2003), Asteriou et al. (2012) are plotted in Fig. 6 with this study. In Chau's results, the specimen with a mass of 204.33 g was selected because that mass is closest to those of our samples. In Asteriou's results, we chose a marble specimen as the reference because marble and limestone have nearly the same hardness. In the absence of detailed data, only the trend line results in the related literature are extracted and redrawn in Fig. 6 to make a comparison. Different line styles are adopted for trend lines in Fig. 6. The lines with data markers are the mean value lines, while those lines without data markers are fitting lines. Two lines, R_v versus the impact angle a for Cagnoli and Manga's test, and R_E versus the impact angle a for Asteriou's test, are absent in Fig 6 because the literature didn't provide them. In addition, ①a and ①b are used to represent results for D=10 cm and D=20 cm in this study, respectively.

Although results of the previous studies and our tests are quite different when they are plotted in one figure, some general trends could be observed. First, all of the trends in R_n versus the impact angle are consistent (see Fig. 6a): R_n decreases with increasing in the impact angle. Asteriou's tests offered the maximum R_n, which can be attributed to the lighter mass and lower impact velocities adopted in the tests. The small R_n values in Cagnoli and Manga's tests were due to the weak strength of pumice whose damage upon impact dissipates kinetic energy, and the impact velocity in this test is much higher than the others. Compared to the other tests, our results produce the steepest descent in the beginning of the trend line. Linear function had been suggested to be used to describe the correlation of R_n and the impact angle α in several reports (Wu, 1985; Richards et al., 2001), although we cannot make a definitive conclusion that linear functions are the best choice. In Fig. 6a, the fitting curve ③ is a second-order polynomial, and the fitting curve ④ is a power function. As mentioned above, it is also found in this study that the best correlation coefficient R^2 is provided by power function when matching data points of R_n.

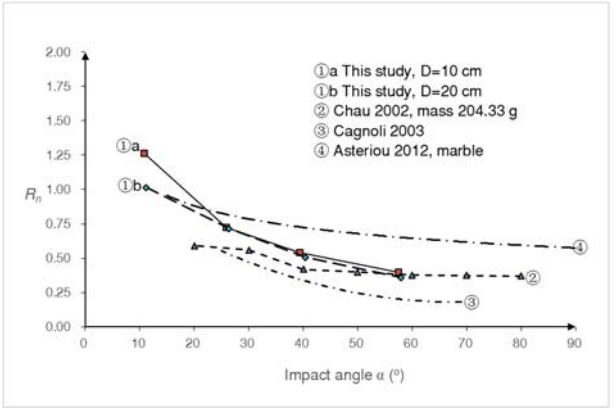

(a) R_n versus the impact angle a

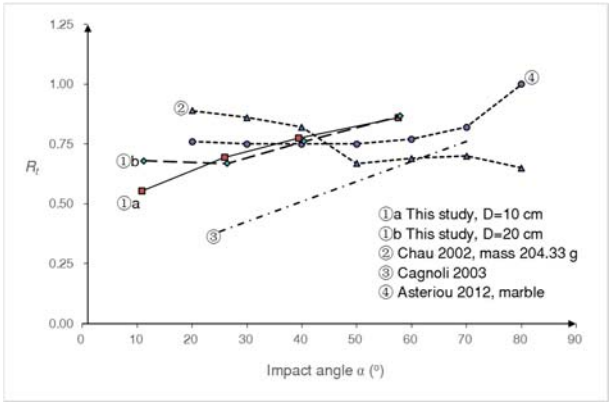

(b) R_t versus the impact angle a

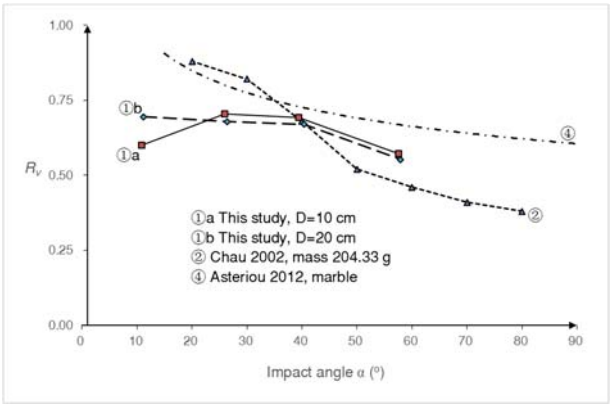

(c) R_v versus the impact angle a

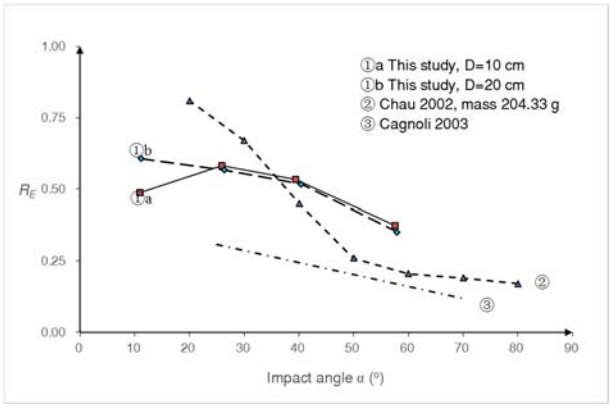

(d) R_E versus the impact angle a

Fig. 6. Comparison with existing small scale experiments

Next, Fig. 6b indicates that the trends of R_t versus the impact angle are scattered. Except for Cagnoli's result, the R_t obtained in the tests are all in the range from 0.5 to 1.0. Wu (1985) suggested that R_t may decrease linearly with increasing in the slope angle θ. In other words, R_t may experience an improvement with increasing in the impact angle α, which is in line with

results of all experiments except Chau's. And Cagnoli and Manga matched data points of R_t using a linear function, which resulted in the fitting curve ④ in Fig. 6b. Therefore, the improvement effect of the impact angle α on R_t is valid in most cases. Besides, when the impact angle is less than 45°, there is an apparent gap between Cagnoli and Manga's result and the other tests. Although the results of the other three experiments are different, the variation ranges of R_t occurs regardless of the test conditions.

Finally, the trends of R_v and R_E versus the impact angle are shown in Fig. 6c and 6d, respectively. Cagnoli and Manga's result is not involved in Fig. 6c for its absence, and for the same reason Asteriou's result is not involved in Fig. 6d. Four unique trend lines are plotted in Fig. 6c, although R_v exhibits a descending trend overall, which means that R_v is reduced in most cases as the impact angle α increases. Similar to R_v, all experiments produce downward trend lines for R_E, except the initial ascent stage in line ①a, which implies that increasing the impact angle induce more kinetic energy dissipation. But, the trend lines in Fig. 6d are scattering. Clearly, the trend lines for R_v and R_E are more likely to be influenced by the test conditions than R_n and R_t. In Fig. 6c the fitting curve ④ is a power function, and in Fig. 6d the fitting curve ③ is a linear function. The difference in the trend lines is apparent for the listed experiments, and we cannot have a conclusion which type of functions should be recommended to match them.

In conclusion, various experimental conditions induce different results for R_n, R_t, R_v and R_E, although there are certain trends that occur regardless of the test conditions. The normal coefficient of restitution R_n, kinematic coefficient of restitution R_v and kinetic energy coefficient of restitution R_E all decrease with increasing in the impact angle, while the tangential coefficient of restitution R_t increases as the impact angle increases in most cases. Power function appears suitable to be used in fitting data points of R_n, while its validity is worth to be further verified by other studies.

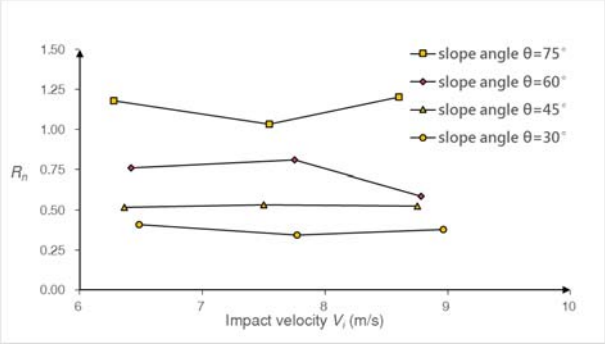

Fig. 7. R_n versus the impact velocity v_i in this study

In addition, Asteriou's test provided the highest trend lines of R_n and R_v in Fig. 6, while Cagnoli and Manga's test provided the lowest trend lines of R_n, R_t and R_E. Asteriou's experiment was conducted using the lowest impact velocity in Table 2, while the highest impact velocity are adopted by Cagnoli and Manga. And Cagnoli and Manga employed pumice, which has a much weaker strength compared to sample materials in other tests. Asteriou and Tsiambaos (2018) has just noticed that R_n reduces when increasing the impact velocity, and increases as the material become harder, which partly accounts for the difference between Asteriou's and Cagnoli and Manga's test. However, we cannot make a definitive conclusion which factor

in Table 2 is the main reason for the magnitude difference in the coefficient of restitution between the tests compared. The tests compared differ from each other in multiple test conditions as Table 2 lists, the estimation of the effect of one specific factor on the magnitude of the coefficient of restitution is unreasonable using their data together. To evaluate the effect of the impact velocity in this study, Fig. 7 plots the mean value of R_n versus the impact velocity with different slope angles. No determined trend appears for the limited variation range of the impact velocity.

4 Direction transitions of translational velocities and rotation

4.1 Direction transitions of translational velocities

The relationship between the impact angle and the rebound angle based on the test results is shown in Fig. 8. Assuming that the falling rock is spherical and that no energy dissipation occurs during the collision, the rebound angle should theoretically be equal to the impact angle, which would result in the data points lying on the $\alpha=\beta$ line in Fig. 8.

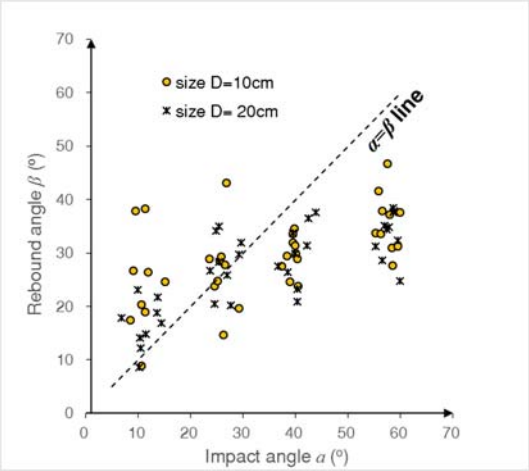

Fig. 8. Rebound angle versus impact angle

However, the test results are almost entirely located above the line in the first impact angle interval, and nearly 50% of the test results are above the line in the second interval. The data points are stably located above the line until the impact angle reaches to 36°. A rebound angle greater than the impact angle was also observed by Cagnoli and Manga (2003), which does not violate the energy dissipation rule. The experimental results presented in Section 3.1 demonstrated that in this study the kinetic energy loss constituted 40-65% of the total kinetic energy for many data points in the first impact angle interval, and constituted 35-55% in the third interval. Therefore, the ratio between the rebound angle and the impact angle cannot be directly used as a reference in estimating whether the energy loss level is high or low.

This phenomenon implies that the rebound motion probably has an unexpected direction of translational velocity. Fig. 9 plots the direction transition of translational velocity caused by the impact, in which diagrams are individually drawn for four impact angle intervals. For a uniform expression, the landing plate is denoted as the bottom black line. Although the

impact velocity directions are concentrated for each impact angle interval, the rebound velocity directions vary considerably. The variation for the interval 36°<α< 44° is the smallest of all intervals.

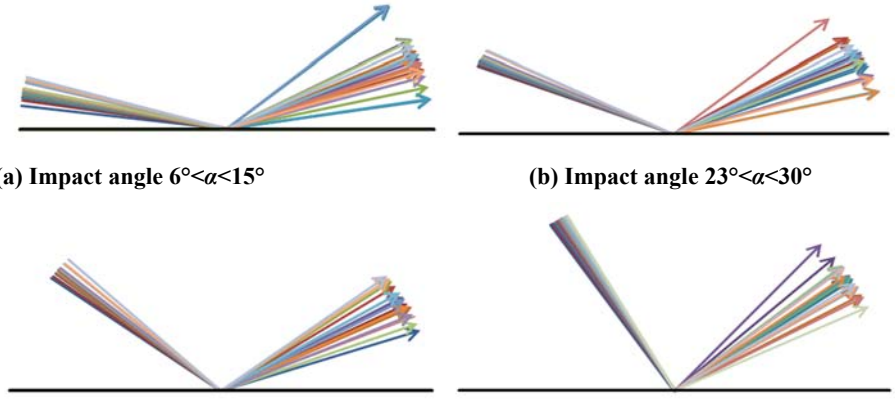

(a) Impact angle 6°<α<15° **(b) Impact angle 23°<α<30°**

(c) Impact angle 36°<α<44° **(d) Impact angle 55°<α<60°**

Fig. 9. Direction transitions of translational velocities induced by impacts

4.2 The rotation caused by the impact

Except the direction transition of translational velocity, the rotation is another significant consequence of the impact. Despite little rotation before impact, the samples occurred an observable rotation after impact in this study, and the angular velocities were recorded and involved in the calculation of the kinetic energy coefficient of restitution R_E. Considering that the magnitudes of kinetic energy before impact varied in this study, the percentage between E_{rr} and E_i is used to denote how much kinetic energy is dissipated in rotation after the impact. As mentioned in Section 1.1, E_i is the total kinetic energy before impact, and E_{rr} is the rotation energy after impact.

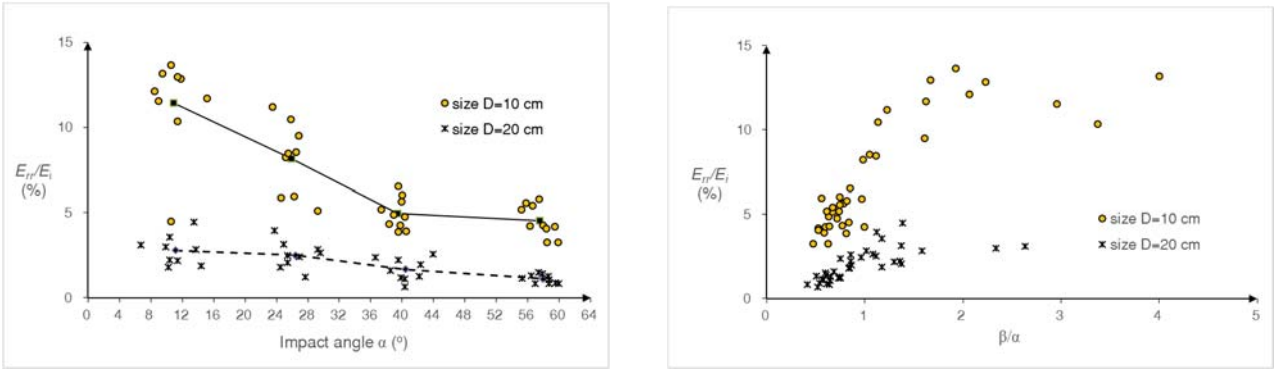

(a) E_{rr}/E_i versus the impact angle **(b) E_{rr}/E_i versus β/α**

Fig. 10. Rotational energy caused by the impact

Fig. 10a shows the effect of impact angle on E_{rr}/E_i. A solid line represents the mean values for specimens with size D=10 cm, while a dashed line is for size D=20 cm. At firstly, the difference is most remarkable between two sample sizes in Fig. 10a.

E_{rr}/E_i ranges from 3.3% to 13.7% for size D=10 cm, and ranges from 0.7% to 4.5% for size D=20 cm, which means that small samples are more likely to have a high E_{rr}/E_i than larger samples. Next, E_{rr}/E_i reduces as the impact angle increases. For size D=10 cm, E_{rr}/E_i experiences a steep decline from the first impact angle interval to the third, then decreases gently to the fourth. For size D=20 cm E_{rr}/E_i has a gradual reduction all the time, which may be attributed to its small variation range. At last, the improvement of the impact angle results in more concentrated data points, although data points for size D=10 cm are always more scattering than size D=20 cm. Both the impact angle and the sample size have an important impact on E_{rr}/E_i in this study. In conclusion, larger samples are more likely to have a stead and small E_{rr}/E_i than small samples, and a large impact angle leads to a small E_{rr}/E_i.

As mentioned in Section 4.1, the unexpected direction transition of translational velocity always happens when the impact angle is small. The correlation between the direction transition of translational velocity and E_{rr}/E_i is investigated by using β/α (the ratio between the rebound angle and the impact angle) as a reference. Fig. 10b illustrated the trends for E_{rr}/E_i versus β/α. E_{rr}/E_i increases as the ratio β/α increases. If β/α is smaller than 1.0, E_{rr}/E_i are much concentrated, which ranges from 3.3% to 6.5% for size D=10 cm and ranges from 0.7% to 2.6% for size D=20 cm. With increasing in β/α, the data points become scattering. Moreover, the improvement of E_{rr}/E_i appears being terminated when β/α reaches a specific value. So, we can have a conclusion that a strong correlation occurs between E_{rr}/E_i and β/α. For a given impact angle, larger rebound angles means that more kinetic energy be converted to rotational energy during the collision.

4.3 The correlation between the coefficients of restitution and the rotation

The rotation plays an important role in energy dissipation during impact, especially for small samples. The percentage between the resulting rotational energy and the original total kinetic energy decreases as the impact angle increases. The correlation between E_{rr}/E_i and the coefficients of restitution is investigated in this section, to evaluate the effect of rotation.

Fig. 11 plots the coefficients of restitution versus E_{rr}/E_i for this study. The four coefficients fall into two categories according to their responses to E_{rr}/E_i. The first category includes R_n and R_t, two most commonly used coefficients of restitution, which appears a strong correlation with E_{rr}/E_i. As E_{rr}/E_i increases, R_n increases but R_t decreases, which verified Broili's deduction (1973). The rotation generated from impact results in an increased normal velocity and reduced tangential velocity. Furthermore, more kinetic energy are converted to rotational energy during the collision, higher R_n and lower R_t we will have. In Fig. 11a and 11b, data points for two sizes are not mixed, which can be attributed to the effect of sample sizes on the magnitude of E_{rr}/E_i. Besides that, data points become more scattering with increasing in E_{rr}/E_i. Various functions have considered to match data points of R_n and R_t, and power function provides the best fitting curve, which has a correlation coefficient R^2 more than 0.65 (except R_t for size D=20 cm). R_v and R_E belong to the second category. There is no remarkable correlation between them and E_{rr}/E_i as shown in Fig. 11c and 11d, so R_v and R_E are independent of the rotation motion in this study. In conclusion, the improvement in the percentage of kinetic energy converted to rotational energy leads to large R_n and small R_t, while it has no distinct influence on R_v and R_E.

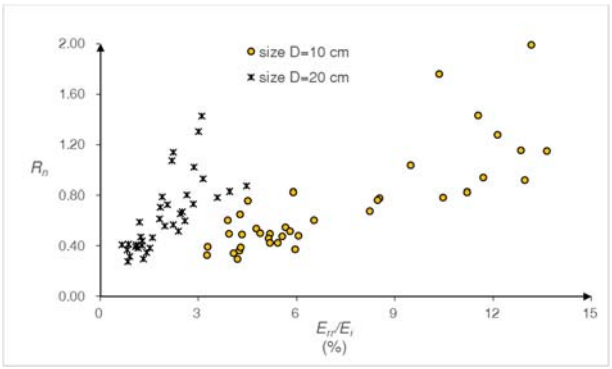

(a) R_n versus E_{rr}/E_i

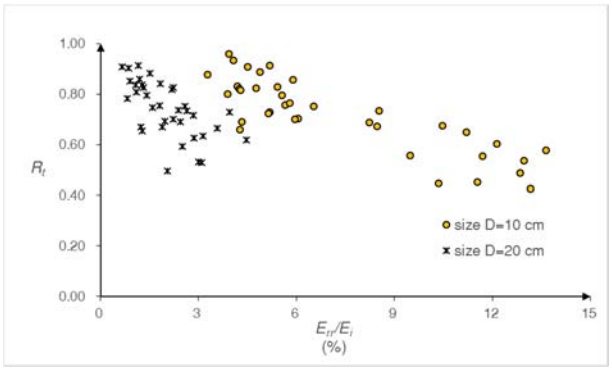

(b) R_t versus E_{rr}/E_i

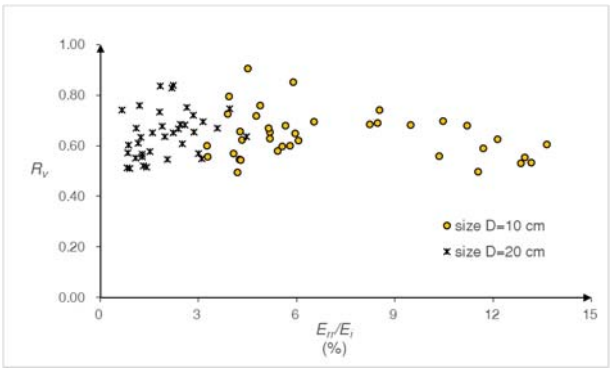

(c) R_v versus E_{rr}/E_i

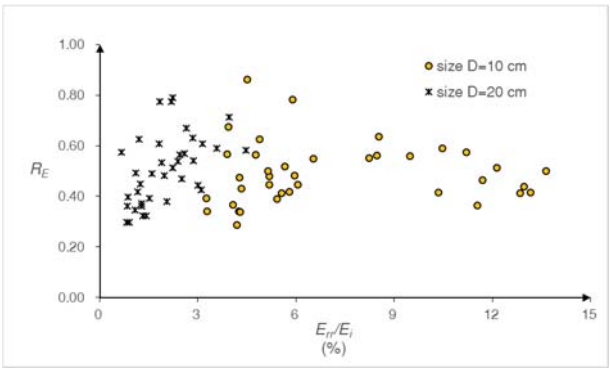

(d) R_E versus E_{rr}/E_i

Fig. 11. The influence of E_{rr}/E_i on the coefficients of restitution

As illustrated in Fig. 10a, more kinetic energy is converted to rotational energy during the collision with a smaller impact angle. Considering the effect of E_{rr}/E_i on R_n and R_t, a smaller impact angle is more likely to have a high R_n and a low R_t than a larger impact angle. Therefore, R_n typically decrease with increasing in the impact angle, and R_t increases as the impact angle increases. When the impact angle is small, two sample sizes appear a clear distinction in E_{rr}/E_i as shown in Fig. 10a, which results in the difference in the mean values of R_n and R_t between two sizes in the first impact angle interval in Fig. 5a and 5b.

5 Discussion

5.1 The main reason for the high rebound angle in case small impact angles

The rebound angle is easier to be larger than the impact angle when the impact angle is small, which can be associated with the impact orientation and the damages caused by the impact. The sample has irregular cutting facets and rear edges in this study, while the landing plate was made of concrete slabs of a smaller hardness compared to the falling samples. When the spherical polyhedron impacts the landing plate with a corner contact or an edge contact, the damages will happen. Fig. 12a

shows the indentations on the surface caused by the impacts. The configuration of indentation is simplified as Fig. 12b to address the effect of the indentation on the rebound angle.

Once the impact compression ends, the indentation is formed completely and the rebound motion starts. The rebound angle is constrained by the border of the resulting indentation. The restriction is less susceptible to the small rebound angle, because a translational motion along the dashed arrow indicates additional penetration. Theoretically, the rebound angle will be less than the impact angle accounting for energy loss. When the impact angle is sufficiently large to generate a rebound angle as the solid arrow, the border imposes no constraints on the rebound motion, and the sample can leave with the default rebound angle. But, when the impact angle is small and generate a default rebound angle as the dashed arrow, rotation motion must be involved to overcome the constraint. Therefore, the penetration caused by the impact may contribute to the large rebound angle under small impact angles.

(a) Indentations caused by the impacts

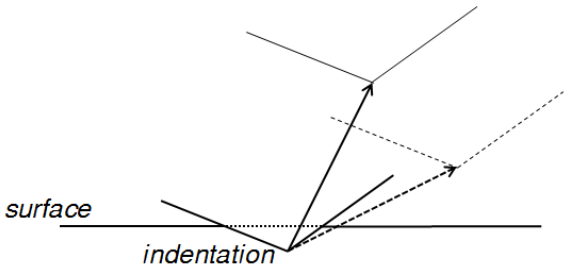

(b) Simplified configuration of indentation and its restriction on motion

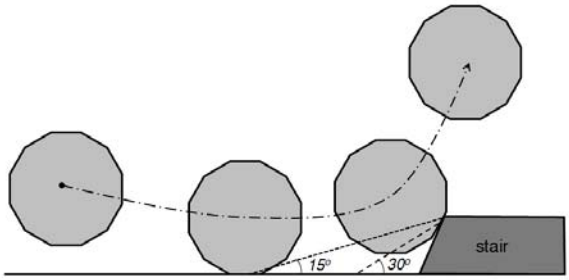

(c) Effect of macro roughness on the rebound angles

Fig. 12. Effect of indentation on the rebound angles

Another important factor to generate the larger rebound angles is the macro roughness of the landing plate, which comes from repeated damages on the slab surface. Assuming that the macro roughness of the landing plate is represented as a small stair in Fig. 12c, the interaction between the falling sample and surface may have two stages in certain situations. The sample impacts the surface before the stair and starts leaving in the first stage. Then, the sample contacts the stair and the velocity changes again in the second stage. The time interval between the two stages is sufficiently short that the two stages appear to finish simultaneously. For the velocity changed by the stair is treated as the rebound velocity, the rebound angle is greater

than the impact angle. Given a fixed stair, the impact angle determines whether the two-stage interaction occurs. Considering that a small impact angle will, in theory, induce a smaller rebound angle, it will increase the risk of the sample contacting the stair when leaving the surface. As illustrated in Fig. 12c, if the default rebound angle is 15°, the stair can affect the rebound behaviour if the sample contacts the surface within 3.73 times the stair height before the stair. As the default rebound angle increases, the surface region that the stair can affect the rebound behaviour decreases.

So, the restriction from the configuration of the indentation, as well as the macro roughness caused by repeated damages, are more likely to affect the rebound motion when the impact angle is small. As a consequence, the rebound angle is easy to exceed the impact angle under small impact angle, and an unexpected direction of translational velocity occurs.

5.2 Interpretation of normal coefficient of restitution R_n larger than 1.0

Of the various consequences of the rebound angle being greater than the impact angle, high values of the normal coefficient of restitution R_n may be remarkable. Engineers usually take 1.0 as the upper bound of R_n in computer codes, whereas several scholars had reported R_n values larger than 1.0 (Azzoni et al., 1992; Paronuzzi 2009; Spadari et al., 2012). In this section the relationship between R_n and the direction transition of translational velocity is investigated.

Considering that the rotation before impacting is little in this study, the normal coefficient of restitution R_n can be expressed as Eq. (5) based on the basic definition in Section 1.1.

$$R_n = v_{nr} / v_{ni} = \sqrt{E_{rt} / E_{it}} \times \left(\sin\beta / \sin\alpha\right) = \sqrt{E_{rt} / E_i} \times \left(\sin\beta / \sin\alpha\right) \tag{5}$$

By introducing an angle coefficient

$$\lambda = \sin\beta / \sin\alpha \tag{6}$$

Eq. (6) can be simplified as

$$R_n = \lambda\sqrt{E_{rt} / E_i} \tag{7}$$

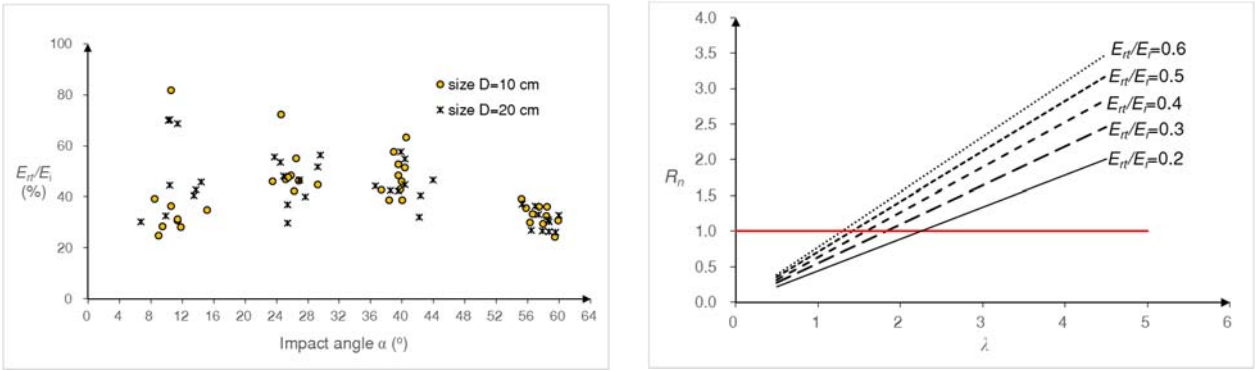

(a) E_{rt}/E_i versus the impact angle **(b) R_n versus the angle coefficient λ**

Fig. 13. The conditions of R_n larger than 1.0

E_{rt}/E_i, the ratio between the translational energy after impacting and the total kinetic energy before impacting, is plotted in Fig 13a with respect to the impact angle. From the perspective of the mean value, as the impact angle increases, when the

impact angles are less than 36° E_{rt}/E increases, and if the impact angles beyond 36°, E_{rt}/E_i decreases. While, the peak values of E_{rt}/E of the four impact angle intervals fall down gradually as the impact angle increases. In this study, the values of E_{rt}/E_i are located in the range (0.20, 0.60) except a few data points, which provides a standard for us to explore the conditions of R_n larger than 1.0.

Fig. 13b plots the relationship between R_n and the angle coefficient λ under different E_{rt}/E_i. The value of R_n increases when increasing the angle coefficient λ. Even if E_{rt}/E_i is only 0.2, R_n is greater than 1.0 when λ>2.24. An extremely large rebound angle is not needed to generate such a λ when the impact angle is small. For example, when the impact angle is 12° and 15°, a rebound angle of 27.8° and 35.5° is sufficient to obtain λ>2.24. Assuming that E_{rt}/E_i is unchanged, a case where the rebound angle is larger than the impact angle must lead to a higher R_n. Although the value of λ corresponding to R_n=1.0 varies with E_{rt}/E_i, the condition λ>1.0 is required to obtain a R_n greater than unity. As shown in Fig. 13b, R_n cannot exceed 1.0 if the rebound angle is lower than the impact angle. As discussed in previous sections, small impact angles are easy to result in unexpected large rebound angles. If the angle coefficient λ formed by the rebound and the impact angle is sufficiently large, R_n will exceed unity even though E_{rt}/E_i is small. Furthermore, assuming a constant E_{rt}/E_i, the reduction in the impact angle decreases the threshold value of the rebound angle that should be satisfied to achieve an R_n in excess of unity, which means that smaller impact angles are more likely to yield a high R_n.

5.3 Relation between the normal coefficient of restitution and the kinetic energy loss

The normal coefficient of restitution R_n has generally been associated with the degree of energy loss due to the elastic-plastic response of the surface material. While, in this study the test results verified that it is unreasonable to simply treat a higher R_n as a symbol of lower kinetic energy loss. Stronge (1991) has pointed out that in the valuation of kinetic energy dissipation, the normal coefficient of restitution is only valid for nonfrictional collisions. For frictional collisions, the total kinetic energy may have a paradoxical increase, if the normal coefficient of restitution is adopted as the unique reference. As shown in Fig. 14, the correlation between R_n and R_E is more complicated in this study, which verifies Stronge's argument.

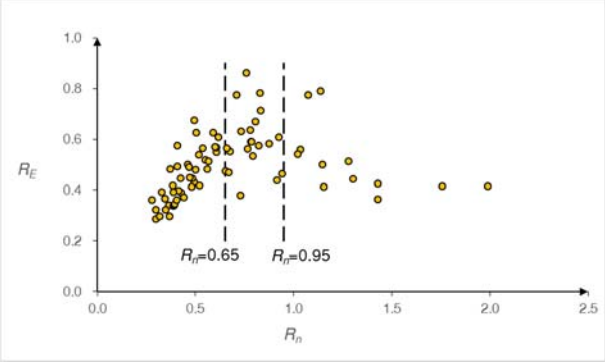

Fig. 14. R_E versus R_n

Increasing R_n will increase R_E initially but decrease it overall. For simplicity, two boundaries (R_n=0.65 and R_n=0.95) are added in Fig. 14. The kinetic energy coefficient of restitution R_E increases with increasing R_n when R_n<0.65, in agreement

with the relationship between R_n and the energy loss level based on the elastic-plastic response analysis. If R_n is greater than 0.95, a larger R_n indicates a smaller R_E. High values of R_n are associated with unexpected rebound angles in this study, which means that the unexpected rebound angles can be related to higher level of kinetic energy loss. R_E is disordered if R_n lies in (0.65, 0.95), which is caused by the two different trends meeting. Therefore, the normal coefficient of restitution cannot be directly used in the evaluation of the kinetic energy dissipation level.

6 Conclusions

The coefficients of restitution are critical parameters in the predication of rockfall trajectory by computer codes. Both the terrain characteristics and kinematic parameters can significantly affect the coefficients of restitution. The effect of the impact angles on the coefficients of restitution have been observed and some laws have been concluded in a series of tests. Until now, the existing laboratory tests have largely been limited to small scale tests, and whether the previous conclusion is valid for different scale tests is uncertain. The role of rotation is still unresolved in the effect of the impact angle on the coefficient of restitution.

In the present study, laboratory tests were performed using a 3D motion capture system. Spherical limestone polyhedra with diameters of 10 cm and 20 cm were taken as samples, and C25 concrete slabs were adopted to form the landing plate. By altering the release height and the inclined angle of the landing plate, the effects of the impact angle on the coefficients of restitution were estimated under freefall test conditions. The result comparison between our test and the existing small scale tests indicated that several general laws occur when accounting for the effect of the impact angle, regardless of the test scales and conditions. The normal coefficient of restitution R_n, the kinematic coefficient of restitution R_v and the kinetic energy coefficient of restitution R_E all decrease when increasing the impact angle, while tangential coefficient of restitution R_t increases as the impact angle increases in most cases. However, the reason for the magnitude difference in the coefficients of restitution between the tests compared is unidentified, for the tests differ from each other in multiple test conditions. When describing the correlation of R_n and the impact angle α, power function may be a better choice than linear function.

When the impact angle is less than 30°, the rebound angle is more likely to exceed the impact angle, which can be attributed to the indentations and macro roughness caused by the impacts. The unexpected direction transition of translational velocity during the collision is always accompanied by the observable rotation. The percentage of kinetic energy converted to rotational energy increases as the impact angle decreases, and large samples are more likely to have a stead and small percentage than small samples. The percentage can be associated with the ratio between the rebound angle and the impact angle. For a given impact angle, larger rebound angles means more kinetic energy be converted to rotational energy during the collision. A higher percentage of kinetic energy converted to rotational energy always induces a higher normal coefficient of restitution R_n and a lower tangential coefficient of restitution R_t, which means that the rotation motion play important role in the effect of the impact angle on the coefficient of restitution. But, no correlations are observable between the rotation motion and the other two coefficients, Rv and R_E.

Whether the rebound angle greater than the impact angle happens is also influenced by the impact orientation, and the impact angle determines its probability. The probability increases as the impact angle decreases, which leads to higher peak values of R_n, as well as the extreme discreteness in the measured data points under small impact angle condition. This issue induces more trouble in rockfall simulations using the normal and tangential coefficients of restitution. If the impact angle is small, the variation range of the coefficient of restitution is large, particularly for R_n, which means that using the typical value in the simulation is unreliable. The stochastic model may be more appropriate for analysing rockfall hazard (Jaboyedoff et al., 2005; Frattini et al., 2008; Bourrier et al., 2009; Andrew and Oldrich, 2017) because it can account for the variation of the restitution coefficient based on data collection. A database of the coefficients of restitution from various experiments should be established to develop more robust stochastic rebound algorithms.

Acknowledgements

Sponsored by Research Fund for Excellent Dissertation of China Three Gorges University, the Open Research Programme of the Hubei Key Laboratory of Disaster Prevention and Mitigation (No. 2017KJZ03), the National Natural Science Funds (No. 51409150), and the CSC Scholarship (No. 201707620009).

References

Agliardi, F. and Crosta G. B.: High resolution three-dimensional numerical modelling of rockfalls. Int J Rock Mech Min Sci, 40, 455–471, 2003

Andrew, M., and Oldrich, H.: Theory and calibration of the Pierre 2 stochastic rock fall dynamics simulation program, Can. Geotech. J., 54(1), 18-30, 2017

Asteriou, P., Saroglou, H. and Tsiambaos, G.: Geotechnical and kinematic parameters affecting the coefficients of restitution for rock fall analysis, Int J Rock Mech Min Sci, 54, 103-113, 2012

Asteriou, P. and Tsiambaos, G.: Effect of impact velocity, block mass and hardness on the coefficients of restitution for rockfall analysis, Int J Rock Mech Min Sci, 106, 41-50, 2018

Azzoni, A., Drigo, E., Giani, G., Rossi, P. and Zaninetti, A.: In situ observation of rockfall analysis, in: Proceedings of the 6th international symposium on landslides, Christchurch, 307–314, 1992

Azzoni, A., Barbera, G. L. and Zaninetti, A.: Analysis and prediction of rockfalls using a mathematical model. Int J Rock Mech Min Sci, 32, 709–24, 1995

Bourrier, F., Dorren, L., Nicot, F., Berger, F. and Darve F.: Toward objective rockfall trajectory simulation using a stochastic impact model, Geomorphology, 110, 68-79, 2009

Bozzolo, D. and Pamini, R.: Simulation of rock falls down a valley side, Acta Mech, 63, 113–30, 1986

Broili, L.: In situ tests for the study of rockfall, Geol Appl Idrogeol, 8, 105–111, 1973

Buzzi, O., Giacomini, A. and Spadari, M.: Laboratory investigation on high values of restitution coefficients, Rock Mech Rock Eng, 45, 35–43, 2012

Cagnoli, B. and Manga, M.: Pumice-pumice collisions and the effect of the impact angle, Geophysical Research Letters, 30, 12, 1636, doi:10.1029/2003GL017421, 2003

Chau, K. T., Wong, R. H. C. and Wu, J. J.: Coefficient of restitution and rotational motions of rockfall impacts, Int J Rock Mech Min Sci, 39, 69–77, 2002

Chau, K. T., Wong, R. H. C., Liu, J., Wu, J. J. and Lee, C. F.: Shape effects on the coefficient of restitution during rockfall impacts, in: Ninth International Congress on Rock Mechanics, ISRM Congress, Paris, 541–544, 1999

Christen, M., Bartelt, P., and Gruber, U.: RAMMS – a modelling system for snow avalanches, debris flows and rockfalls based on IDL, Photogrammetrie, Fernerkundung, Geoinformation, 4, 289–292, 2007.

Dorren, L. K. A.: A review of rockfall mechanics and modelling approaches, Progress in Physical Geography, 27 (1), 69–87, 2003

Dorren, L. K. A., Berger, F. and Putters, U. S.: Real-size experiments and 3-D simulation of rockfall on forested and non-forested slopes, Natural Hazards and Earth System Sciences, 6, 145-153, 2006

Dorren, L. K. A.: Rockyfor3D revealed-description of the complete 3D rockfall model, ecorisQ paper, http://www.ecorisq.org, 2010

Farin, M., Mangeney, A., Toussaint, R., Rosny, J., Shapiro, N., Dewez, T., Hibert, C., Mathon, C., Sedan, O. and Berger, F.: Characterization of rockfalls from seismic signal: Insights from laboratory experiments, J. Geophys. Res. Solid Earth, 120, 7102–7137, 2015

Fornaro, M., Peila, D. and Nebbia, M.: Block falls on rock slopes-application of a numerical simulation program to some real cases, in: Proceedings of the 6th international IAEG congress, 2173-2180, 1990

Frattini, P., Crosta, G. B., Carrara, A. and Agliardi, F.: Assessment of rockfall susceptibility by integrating statistical and physically-based approaches, Geomorphology, 94 (3-4), 419-437, 2008

Giani, G. P.: Rock Slope Stability Analysis, Rotterdam, Balkema, 1992

Giani, G. P., Giacomini, A., Migliazza, M. and Segalini, A.: Experimental and theoretical studies to improve rock fall analysis and protection work design, Rock Mech Rock Eng, 37(5), 369–389, 2004

Guzzetti, F., Crosta, G., Detti, R. and Agliardi, F.: STONE: a computer program for the three dimensional simulation of rock-falls, Computer & Geosciences, 28, 1079–1093, 2002

Guzzetti, F., Reichenbach, P. and Wieczorek, G. F.: Rockfall hazard and risk assessment in the Yosemite Valley, California, USA, Natural Hazards and Earth System Sciences, 3, 491-503, 2003

Habib, P.: Note sur le rebondissement des blocs rocheux, in: Rockfall dynamics and protective works effectiveness, ISMES publication, 90, 123–125, 1976.

He, S. M., Wu, Y. and Yang, X. L.: Study of rock motion on slope, Chinese Journal of rock mechanics and engineering, 27(s1), 2793-2798, 2008

Heidenreich, B.: Small- and half-scale experimental studies of rockfall impacts on sandy slopes, PhD Thesis, Ecole Polytechnique Fédérale de Lausanne, Swiss, 2004

Jaboyedoff, M., Dudt, J. P. and Labiouse V.: An attempt to refine rockfall zoning based on kinetic energy, frequency and fragmentation degree, Natural Hazards and Earth System Sciences, 5, 621–632, 2005

James, G.: Rock-shape and its role in rockfall dynamics, PhD Thesis, Durham University, 2015

Jones, C., Higgins, J. D. and Andrew, R. D.: Colorado Rockfall Simulation Program User's Manual for Version 4.0, Denver: Colorado Department of Transportation, 2000

Pappalardo, G., Mineo, S. and Rapisarda, F.: Rockfall hazard assessment along a road on the Peloritani Mountains (northeastern Sicily, Italy), Natural Hazards and Earth System Sciences, 14, 2735-2748, 2014

Paronuzzi, P.: Probabilistic approach for design optimization of rockfall protective barriers, Quarterly Journal of Engineering Geology, 22, 175–183, 1989

Paronuzzi, P.: Field evidence and kinematical back analysis of block rebounds: the Lavone rockfall, Northern Italy, Rock Mech Rock Eng, 42, 783–813, 2009

Richards, L. R., Peng, B. and Bell, D. H.: Laboratory and field evaluation of the normal coefficient of restitution for rocks, in: Proceedings of Eurock, 149–156, 2001

Robotham, M. E., Wang, H. and Walton, G.: Assessment of risk from rockfall from active and abandoned quarry slopes. Transactions - Institution of Mining & Metallurgy, Section A.104, A25–A33, 1995

Scioldo, G.: User guide ISOMAP & ROTOMAP-3D surface modelling and rockfall analysis, Geo & Soft International, 2006

Spadari, M., Giacomini, A., Buzzi, O., Fityus, S. and Giani, G.: In situ rock fall tests in New South Wales, Australia, Int J Rock Mech Min Sci, 49, 84-93, 2012

Stevens, W.: RockFall: a tool for probabilistic analysis, design of remedial measures and prediction of rock falls, Master thesis, University of Toronto, 1998

Stronge, W. J.: Friction in collisions: Resolution of a paradox, Journal of Applied Physics, 69, 610-612, 1991

Valentin, S. G., Oldrich, H., Andrew, M., and Franck B.: Pierre3D: a 3D stochastic rockfall simulator based on random ground roughness and hyperbolic restitution factors, Can. Geotech. J., 52, 1360-1373, 2015

Wu, S. S.: Rockfall evaluation by computer simulation, Transportation Research Record, Transportation Research Board, Washington DC, 1031, 1–5, 1985